PHASE TRANSFORMATIONS IN NICKEL-BASE SUPERALLOYS

J. R. Mihalisin and D. L. Pasquine

Abstract

A study has been made of the phase transformations that occur during long time rupture testing of IN-731X, an alloy specifically designed for phase stability. No sigma formation was observed in this alloy.

The beneficial effect of heat treatment in inhibiting sigma formation and the anomalous effect of heat treatment on the rupture properties of alloy 713C and alloy 713LC have been correlated with microstructural alterations induced by heat treatment.

A method for electron vacancy calculation has been devised which incorporates the actual γ' chemistry obtained by preferential extraction techniques and chemical analysis. This method is used to show that long time rupture testing and heat treatment have little effect on electron vacancy number.

J. R. Mihalisin and D. L. Pasquine are with The International Nickel Company, Inc., Paul D. Merica Research Laboratory, Sterling Forest, Suffern, New York 10901

INTRODUCTION

A recent study(1) has shown how compositional modification of IN 100 alloy leads to freedom from sigma formation. A new alloy, IN-731X, has been developed which incorporates these changes without sacrificing IN 100 alloy properties.

The above study also revealed that a certain heat treatment reduced sigma susceptibility in alloy 713C and alloy 713LC. However, this treatment had an anomalous effect on properties; being beneficial for alloy 713LC, but detrimental to alloy 713C's 1500°F rupture strength.

In the present study, the phase transformations in IN-731X have been delineated. The effect of heat treatment on the phase transformations and phase morphology in alloys 713C and 713LC have been correlated with properties. The electron vacancy concept was used in these investigations but was extended beyond its usual simplifying assumptions by employing actual γ' phase compositions.

EXPERIMENTAL PROCEDURE

Phase transformations were studied by light and electron microscopy and x-ray diffraction.

Specimens for light microscopic examination were prepared by conventional grinding and polishing followed by etching with glyceregia (2:1 HCl/HNO_3 + 3 glycerine by volume). Photomicrographs of stress rupture specimens were taken adjacent to the fracture.

Negative replicas for electron microscopy were taken from surfaces electropolished with a solution of 15% H_2SO_4 in methanol and etched in glyceregia.

X-ray diffraction studies of carbide phases were made from residues electrolytically extracted in 10% HCl in methanol. The γ' phase was electrolytically extracted in a solution of 20% H_3PO_4 in H_2O and was shown, by x-ray diffraction examination, to be free of contamination from other phases. The composition of the γ' phase was determined by wet chemical analysis. X-ray diffraction studies were made with iron-filtered CoKα radiation. X-ray patterns were recorded using a goniometer speed of 1/2°/minute. The scintillation counter and pulse height analyzer operated at a channel height of 10 volts and a channel width of 12 volts. The equipment was calibrated with a powdered gold standard.

RESULTS AND DISCUSSION

I. Alloy IN-731X

The results of stress rupture tests on IN-731X in the temperature range of 1350°F to 1900°F are shown in Figure 1. The material was tested as cast and with two grain sizes. The coarse grains averaged 1/4" diameter while the fine grains averaged 1/8" in diameter. The chemical composition of this heat is given in Table I which also shows the compositions of the other heats used in this study.

A compilation of the various phases electrolytically extracted from some of the test specimens of Figure 1 is given in Table II. In the "as cast" condition the major secondary phase is MC carbide with a lattice parameter equal to 4.30Å. This value is in excellent agreement with previous parameter data for pure TiC (2). The major phase change taking place in the alloy is a gradual formation of $M_{23}C_6$ carbide in the temperature range of 1350°F to 1900°F. This change is time-temperature dependent. At 1350°F $M_{23}C_6$ formation takes a longer time than at 1900°F. Also, at least as shown by the data at 1800-1900°F, the $M_{23}C_6$ carbide forms at the expense of the MC carbide. There is little change in the lattice parameters of these phases under the test conditions employed. In addition, the phase transformations are identical in both coarse- and fine-grained alloys.

Figure 1 shows that the coarse grain condition results in a higher rupture strength in the 1800 to 1900°F region; the effect becoming most prominent at 1900°F. At 1700°F the fine grain alloy has a higher rupture strength whereas little effect of grain size on strength is noticed at 1350 and 1500°F. The grain boundary morphology is similar for both coarse and fine grain alloys as shown by the micrographs of Figure 2 for specimens tested at 1800°F. It seems likely therefore that the higher strength of the coarse grain material at higher temperature is simply a grain size effect unrelated to the phase transformations taking place.

An electron vacancy computation, $\overline{N}_V$ (ref), yields a value of 2.31. This method of $\overline{N}_V$ computation is given in Appendix I and will be referred to as $\overline{N}_V$ (ref) throughout this discussion. This method of electron vacancy computation has been agreed upon as the standard method to be used for comparison purposes at the International Symposium on Structural Stability at Seven Springs, Pennsylvania. ($\overline{N}_V$ (ref) values for the alloys are listed in Table I). Alloys with $\overline{N}_V$ numbers less than about 2.50 are considered not to be prone to sigma formation. However, sigma has been found in alloys of the Alloy 713C type with $\overline{N}_V$ numbers as low as 2.10(1). No sigma was detected in the IN-731X alloy studied here.

The most questionable assumption made in conventional $\overline{N}_V$ computations lies in the treatment of the γ' precipitation. First of all, it is usually assumed that all aluminum and titanium in the alloy is used to form γ', ($Ni_3(Al, Ti)$). From a consideration of simple Ni-Al-Ti alloys(3) (upon which system complex superalloys are based), it can readily be seen that aluminum and titanium are actually partitioned between the γ and γ' phases as γ' precipitates from γ. In addition, the γ' phase in superalloys has some solubility for many other alloying additions, as demonstrated by Guard and Westbrook(4). When these effects are taken into account, it is clear that the residual matrix composition would differ from that obtained by assuming that γ' is simply Ni_3 (Al, Ti) and that it consumes the total aluminum-titanium content of the alloy. This, of course, would markedly affect the $\overline{N}_V$ number of the alloy, since the residual matrix composition after precipitation has taken place is used to calculate this number.

The chemical composition (in atomic percent) of the γ' phase extracted from an as-cast specimen of IN-731X is given in Table III. The results are an average of two separate determinations. The mean deviation of these from the average is also given. The largest variations are in the aluminum and titanium contents, and this is probably an indication of microsegregation. As can be seen, the γ' phase has solubility for a number of elements. Earlier work(4) indicated that cobalt would inhabit nickel sites in the γ' (Ni_3Al) phase, while Cr and Mo would tend to occupy both nickel and aluminum sites. Titanium and vanadium tend to occupy aluminum sites. Using this as a basis, a formula:

	Ni	Co	Cr	Mo		Al	Ti	V	Cr	Mo
$($	.880	.079	.034	.009	$)_3$	.613	.331	.023	.023	.010

can be deduced for the γ' composition given in Table III. The distribution of chromium and molybdenum between nickel and aluminum sites above is not arbitrary. Measurements of the degree of long range order indicate that chromium and molybdenum inhabit nickel sites in a ratio of approximately four to one. Any remaining chromium and molybdenum occupy aluminum sites. In any event, this is not a critical point in the discussion to follow since it only affects the calculation of the density of the γ' phase and the effect is small because of the small amounts of chromium and molybdenum involved.

Knowing the composition and volume percentage of γ' in the alloy and the density and composition of the alloy, a determination can be made of the residual matrix composition after γ' precipitates from γ.

This is done in the following manner: the weight of the i^{th} element in the residual matrix (γ) is given by:

$$(W_i)^{\gamma} = (W_i)^{\text{alloy}} - \left\{(W_i)^{Cr_{21}Mo_2C_6} + (W_i)^{TiC} + (W_i)^{\gamma'}\right\}$$

where i = Cr, Co, Mo, V, Ti, Al, and Ni

$$(W_i)^{\text{alloy}} = \rho_{\text{alloy}} \times (\text{unit vol}) \times (\text{weight percent of } i^{th} \text{ element in alloy})$$

ρ_{alloy} = density of alloy

$(W_i)^{Cr_{21}Mo_2C_6}$ and $(W_i)^{TiC}$ are weights of respective carbides assuming all carbon is converted to carbide and evenly divided between the two varieties.

$$(W_i)^{\gamma'} = \rho_{\gamma'} \times (\text{volume percent } \gamma') \times (\text{weight percent of } i^{th} \text{ element in } \gamma')$$

$\rho_{\gamma'}$ = density of γ';

$$\rho_{\gamma'} = \frac{\sum_i^{th} \text{atoms on nickel sites} \times (\text{atomic weight})i + \sum_i^{th} \text{atoms on aluminum sites} \times (\text{atomic weight})i}{\text{Avogadro's Number} \times a_o^3}$$

a_o = lattice parameter of γ' phase

$$\text{weight percent of } i^{th} \text{ element in } \gamma = \frac{(W_i)^{\gamma}}{\sum (W_i)^{\gamma}}$$

The weight percent of each element is converted to atomic percent and the formula for $\overline{N}_v$ is calculated as usual:

$$\overline{N}_v = \sum (\text{atomic percent}) \; i^{th} \text{ element} \times (\overline{N}_v)i$$

Using ρ alloy = 7.75 g/cm^3, a_o = 3.58Å and vol % γ' = 58.4 as measured on electron micrographs yields a value of $\overline{N}_v$ = 2.07 which is significantly lower than the $\overline{N}_v$ (ref) value of 2.31.

It was noticed in making this calculation that the amount of titanium left in the residual matrix after precipitation was reduced virtually to zero. This suggested a method of determining the volume percent of the γ' in this alloy without recourse to laborious lineal analysis of micrographs. This could be done by using the relation:

$$(W_i)^{\gamma'} = \rho_{\gamma'} \text{ (volume percent } \gamma') \times (\text{weight percent of } i^{th} \text{ element in the } \gamma')$$

Assuming all titanium is consumed by γ' except that amount precipitated as TiC gives:

$$(\text{volume percent } \gamma') = \frac{(\text{Weight of titanium alloy-weight of Ti in TiC})}{(\text{Weight percent Ti in } \gamma') \times \rho_{\gamma'}}$$

As seen in Table III, the volume percent γ' calculated from such determinations yields an average value of $58.9 \pm 3.8\%$ which is in excellent agreement with the observed value of 58.4%. A typical area of the "as cast" structure is shown in Figure 3.

The average $\overline{N}_v$ value calculated using the assumption that there is no Ti in the residual matrix is also given in Table III. It appears that the reproducibility obtainable for $\overline{N}_v$ by this method is about $\pm$ 0.04 electron vacancy units. It should also be noted that an appreciable amount of aluminum is left in the residual matrix. Following the Pauling scheme, aluminum is given an $\overline{N}_v$ value of 7.66 units for calculation purposes.

Table IV compares the compositions of the γ' and the residual matrix of as-cast IN 731X with those of samples rupture tested at 1350°, 1500°, and 1800°F. The volume percent γ' calculated as shown above (no titanium in the residual matrix) and volume percent γ' measured from electron micrographs are shown along with $\overline{N}_v$ numbers. A formula for γ' is given for each γ' composition on the basis discussed previously. It can be seen that there is excellent agreement between volume percent γ' calculated and volume percent γ' measured which shows that the assumption that titanium is reduced to zero in the residual matrix is a valid one. The $\overline{N}_v$ numbers in Table IV have been calculated on the basis that titanium is reduced to zero in the residual matrix although there is very little difference (within $\pm$ .02 electron vacancy units) if volume percent γ' observed is used instead in the calculations.

It is readily seen that, within experimental error, there is little variation in $\overline{N}_v$ number over a wide range of temperature and stress conditions, and little variation of these from the as-cast value. The only exception is at 1500°F where the $\overline{N}_v$ number was slightly lower. It is thus reasonable to assume that $\overline{N}_v$ number for this alloy can be considered a constant over a wide range of time, temperature, and stress.

It is also seen from the γ' formulas that vanadium tends to take up positions on nickel sites as the temperature of testing is increased. This could be the result of dissolution of TiC at the higher temperatures thus releasing titanium and depriving vanadium of aluminum sites which are now preferentially taken up by titanium. This is also reflected in the increase in titanium content of the γ' in the 1800°F test specimen. Also there is a decrease in the chromium content of the γ' phase particularly in the 1800°F test specimen where extensive $Cr_{21}Mo_2C_6$ formation occurs (Table II) making less chromium available for the γ' phase. There is also a decrease in the volume fraction of γ' phase at 1800°F. This would result in some diminution of strength.

II. Effect of Heat Treatment on Alloy 713C and Alloy 713LC

Previous study(1) of alloys 713C and 713LC has shown that heat treatment can affect subsequent sigma formation. This is illustrated by the data in Table V. It can be seen that, for those alloys which form sigma, a treatment of 2150°F/1 hr. + 1900°F/4 hours reduces the amount of sigma formed at 1500°F.

The effect of heat treatment on the microstructure of alloy 713C is shown in Figure 4. The phases listed under the optical micrographs are the phases identified in electrolytic extraction residues. It is apparent that extensive $M_{23}C_6$ carbide formation occurs after 4 hours at 1900°F while at 2150°F, in one hour, only a small amount of M_6C carbide was formed. The combination treatment (2150°F/1 hr. + 1900°F/4 hrs.) yielded both $M_{23}C_6$ and M_6C carbides. The optical micrographs reveal some alteration in the γ' morphology in the 2150°F heat treated and doubly heat treated samples particularly near grain boundaries.

To study the alterations in morphology in detail of these phases after heat treatment, electron microscopy is necessary. Figure 5 compares the as-cast microstructure of alloy 713C(area(a)) with three areas observed after a treatment of 2150°F for one hour. In area(b) (near a grain boundary), it is apparent that much of the γ' has been dissolved by this treatment and reprecipitated in a "feathery" type distribution. In area(c), near MC carbides, the γ' has a somewhat different distribution but definitely shows evidence of solutioning and reprecipitation. In addition, initiation of precipitation of carbide, presumably M_6C, occurs around MC carbides. In area(d) the γ' has about the same distribution as in the as-cast condition, although this type of area is not as prevalent as areas(b) and (c). This indicates that a short time at high temperature may not be sufficient to completely dissolve γ'.

A similar comparison of the microstructure after a treatment at 1900°F for 4 hours is shown in Figure 6. In area(a), the γ' is similar in appearance to that in the as-cast microstructure, although some has dissolved and reprecipitated. Area(b) shows agglomeration and reprecipitation of γ' similar to that in Figure 5(c). In area(c) extensive carbide formation around MC carbides occurs. Also, although not shown here, there is extensive carbide formation at grain boundaries after this treatment. From the x-ray diffraction data, it would appear that the major amount of this carbide is of the $M_{23}C_6$ type.

The microstructure after the dual treatment (2150°F/1 hr. + 1900°F/4 hrs.) is shown in Figure 7. In area(a) $M_{23}C_6$ carbide has precipitated at a grain boundary and a wide swath of γ' has developed along the boundary. It is also seen that this grain boundary γ' is very likely different somewhat in composition from the γ' developed in the matrix as evidenced by the difference in elevation where cubical matrix γ' particles intersect grain boundary γ' showing a variation in etching behavior; hence, a difference in composition. The grain boundary γ' may be carbon rich, since γ' has some solubility for carbon as pointed out previously(5). In area(b), as one moves away from the grain boundary, there is a transition from the small cubical γ' particles to larger coarsened ones. Throughout the microstructure (areas a and b) there is very finely dispersed γ'. The alteration in γ' morphology at grain boundaries as viewed optically (Figure 4) for this sample is thus the result of the finer distribution of γ' adjacent to the boundary.

The effect of heat treatment on the microstructure of alloy 713LC is similar to that in alloy 713C. Figure 8 shows the as-cast and heat treated microstructures at 500X magnification. The heat treatment produces alterations in γ' morphology which at low magnification occur as patches intergranularly near carbides and to a lesser degree near grain boundaries. At high magnification (Figure 9), typical areas of the as-cast and heat treated samples are shown. As-cast areas, (a) and (b), illustrate the different shapes of the γ' phase at different sections through the sample. After heat treatment, area(c) shows precipitation of $M_{23}C_6$ carbide and γ' at the grain boundary. The matrix γ' near the boundary is in a fine dispersion. Further away from the boundary, area(d), γ' has agglomerated and reprecipitated in a fine dispersion. Thus the microstructure after heat treatment is similar to that observed in alloy 713C. The major difference is one of degree. There is less carbide precipitation in alloy 713LC because of lower carbon content and less γ' is developed at grain boundaries because of this.

The method of using γ' chemistry to determine $\overline{N}_v$ number as outlined previously for IN-731X effectively allows $\overline{N}_v$ to become a function of time and temperature rather than being only a function of the composition of the alloy. It was decided to apply this method to 713C to determine whether $\overline{N}_v$ could be correlated with the beneficial effect of heat treatment in inhibiting sigma formation. The computations were made in the same way as outlined for IN-731X except that the carbides were assumed to be (Cb, Ti)C and $Cr_{21}Mo_2C_6$. In the case of alloy 713C, it was found that columbium was reduced virtually to zero in the residual matrix so that volume percent γ' could be obtained by using the columbium contents of the γ' and the alloy. Titanium is also reduced to small amounts in the residual matrix but the amount remaining is not quite negligible. These data for as-cast alloy 713C and in three conditions of heat treatment are given in Table VI in an analogous manner to that shown for IN-731X (Table IV). The γ' formula was deduced in the same way as for IN-731X. Again x-ray long range order measurements showed that the chromium and molybdenum distribution on nickel and aluminum sites was similar to that of the γ' extracted from IN-731X. The excellent agreement between volume percent γ' calculated, assuming columbium reduced to zero in the matrix, and volume percent γ' measured attests to the validity of this assumption.

The $\overline{N}_v$ value for Heat 85 in the as-cast condition is 2.20 (Table VI) which is somewhat higher than that for $\overline{N}_v$ (ref) of 2.12 but the discrepancy is not as great as with IN-731X. This is due to the fact that the assumption that all the columbium and titanium is tied up as γ' is not too far removed from what really occurs in alloy 713C. Although not all the aluminum is tied up as γ', this is compensated for by the greater amount of nickel left in the residual matrix. The values of the $\overline{N}_v$ numbers for aluminum and nickel and the amount of partitioning of aluminum between γ and γ' are such as to be very nearly compensating in their effect on $\overline{N}_v$. These compensating effects would not be expected to hold true for all alloys as was shown for IN-731X.

There is very little variation of $\overline{N}_v$ values, within experimental error, with heat treatment (Table VI). The experimental error here is assumed to be about the same as with IN-731X, i.e., $\pm$ .04 $\overline{N}_v$ units. Thus this type of electron vacancy calculation does not serve as an indicator for the influence of heat treatment on sigma formation.

The influence of heat treatment on sigma formation in both 713C and 713LC can be rationalized to some extent on the basis of the previous microstructural observations. Two effects occur as these alloys are heat treated in the 1900-2150°F regions. There is solutioning of γ' and precipitation of $M_{23}C_6$ and M_6C carbides. The preponderant carbide is $M_{23}C_6$ at 1900°F and at 2150°F a small amount of M_6C and no $M_{23}C_6$ forms. With solutioning of γ' there is undoubtedly a general

homogenization of the alloy. This in itself would tend to reduce sigma forming tendency of an alloy in which sigma forming elements had segregated.

The carbides, particularly $M_{23}C_6$ which forms in largest quantities upon heat treatment, contain chromium and molybdenum which are effective elements in forming the Ni-Cr-Mo type sigma observed in this alloy. Thus an alloy which is marginally sigma-prone or macro-segregated can be made less so by precipitation of such carbides, thereby reducing the effective matrix content of the alloy in chromium and molybdenum. There is a seeming paradox here since sigma often nucleates on such carbides in the sigma forming region(1). It is possible that the $M_{23}C_6$ carbides formed upon heat treatment at 1900°F differ in composition from those formed at lower temperatures, possibly being richer in molybdenum which has been shown to be a more effective contributor to sigma formation than its normally assigned value of 4.66 would indicate(1). Even assuming no composition difference in the carbides at these temperatures there would be a balance between the matrix composition, amount and distribution of the carbide formed and sigma forming tendency. In this case it would be possible for carbide precipitation either to inhibit or promote sigma formation. The latter effect would occur in an alloy that was extremely prone to sigma formation so that precipitation of carbide would be insufficient to reduce the sigma forming tendency of the matrix to a large extent. The carbides formed upon heat treatment would then act as nuclei for sigma precipitation.

It will be noticed in Table V for alloy 713LC that, in two heats (07 and 17) of material of practically identical $\overline{N}_V$ (ref) number, one formed sigma and one did not. In fact, the non-sigma heat had a higher $\overline{N}_V$ (ref) than the sigma heat. It was decided to apply the method of $\overline{N}_V$ calculation developed here using γ' composition to determine whether this method would serve as a better indicator for sigma precipitation. The results are given in Table VII in the same manner as for alloy 713C. It can be seen that within experimental error, the $\overline{N}_V$ numbers are the same for both heats. In fact, non-sigma heat had a higher $\overline{N}_V$ number as was the case with $\overline{N}_V$ (ref) (Table V). The concentration of Cb in the residual matrix is reduced virtually to zero as was the case with alloy 713C as shown by the good agreement of volume percent γ' calculated with that of volume percent γ' measured. The $\overline{N}_V$ (ref) value for alloy 713LC is smaller than for alloy 713C due to the lower chromium content of the alloy 713LC heats. However, when using the $\overline{N}_V$ calculation based on γ' composition it is seen that alloys 713C and 713LC, have about the same $\overline{N}_V$ value. These $\overline{N}_V$ values are still rather low for what is generally experienced in practice where $\overline{N}_V$ break-off values of 2.50 for sigma formation are usually found. The rationalization for this is that

molybdenum, in this particular system, has a higher $\overline{N}_V$ value than is commonly assigned(1). Using an $\overline{N}_V$ value of 9.66 as developed in (1) yields $\overline{N}_V$'s for alloy 713LC of about 2.40 - 2.45 for $\overline{N}_V$ calculations using actual γ' compositions. This places the alloy nearer the 2.50 break-off value than $\overline{N}_V$ (ref) where using $\overline{N}_V$ = 9.66 for molybdenum yields $\overline{N}_V$'s for alloy 713LC of about 2.25 - 2.30.

It will be noticed (Table V) that although the heat treatment of alloy 713C (2150°F + 1900°F) reduces the tendency to develop sigma, this heat treatment does not appear to have exerted a useful effect on rupture properties at 1500°F. A study was made of these individual heat treatments on structure and these results are shown in Figure 10. As can be seen, each individual heat treatment has reduced the tendency to form sigma, if one ignores the different times at temperature which are not appreciable.

In any event, it is obvious that the rupture properties are not influenced to a great extent by the amount of sigma present. Rather, rupture life correlates with the amount of grain boundary γ' developed in these samples. Little of this grain boundary γ' is developed in the as-cast alloy which had the longest rupture life. More is developed in the heat treated samples, all of which had lower lives than the as-cast material. The greatest amount of γ' formed in the specimen which had been given a dual treatment and which had the lowest life. The previous microstructural studies indicate that this is the result of carbide precipitation at grain boundaries during heat treatment. This induces grain boundary γ' formation. It is possible that the large amount of sigma developed in the as-cast sample prevented precipitation of grain boundary γ' and so increased strength.

On the other hand the data of Table V show that the same heat treatment for alloy 713LC produces an increase in rupture life at 1500°F over the as-cast material. It will also be noticed that the heat with the lowest carbon level (Table I) benefited the most strengthwise from heat treatment. An optical micrograph of this heat is shown in Figure 11 after the 3600-hour test (heat treated condition). It will be seen that little agglomerated γ' can be detected at this magnification at grain boundaries unlike the case for heat treated alloy 713C (Figure 10). It is possible that there is an optimum amount of carbide precipitated at grain boundaries that is useful in increasing rupture strength. However, heat treatment does homogenize and refine the γ' structure which could also be a strengthening mechanism as has been already suggested(5). This strengthening effect could compensate for any weakening effect carbides might have at grain boundaries. In this case, an alloy with as low carbon as possible would derive the greatest strength benefit from heat treatment. Some

carbon might be useful as a means for inhibiting sigma formation by heat treatment, however, and/or as a possible strengthening mechanism through carbide precipitation upon heat treatment.

III. Partitioning of Alloy Elements Between the γ' Phase and the Residual Matrix

The partitioning of elements between γ' and residual matrix in IN-731X, Alloy 713C and Alloy 713LC is shown in Figure 12. The results shown are averages of all the determinations for each alloy presented in this study since there was little significant variation between the different samples from each alloy. The average γ' composition for each of the alloys in formula form is as follows:

IN 731X $(Ni_{.884}\ Co_{.070}\ Cr_{.032}\ Mo_{.008}\ V_{.003})_3\ (Al_{.632}\ Ti_{.347}\ V_{.013}\ Cr_{.006}\ Mo_{.002})$

Alloy 713C $(Ni_{.978}\ Cr_{.017}\ Mo_{.004})_3\ (Al_{.717}\ Cb_{.096}\ Ti_{.052}\ Mo_{.036}\ Cr_{.102})$

Alloy 713LC $(Ni_{.983}\ Cr_{.014}\ Mo_{.004})_3\ (Al_{.711}\ Cb_{.102}\ Ti_{.044}\ Mo_{.040}\ Cr_{.104})$

There is little difference between the γ' composition of alloys 713C and 713LC so that an average value can be used for both alloys as follows:

$(Ni_{.980}\ Cr_{.016}\ Mo_{.004})_3\ (Al_{.714}\ Cb_{.099}\ Ti_{.048}\ Mo_{.038}\ Cr_{.103})$

Nickel (Figure 12) is preferentially concentrated in the γ' phase for all three alloys, but a large amount remains in the residual matrix. The absolute level is higher in 713C and 713LC than in 731X because of the cobalt present. Titanium is concentrated in the γ' phase in all three alloys but to a greater extent in IN-731X (practically all of it) than in alloys 713C and 713LC. Aluminum is concentrated in the γ' phase in all three alloys but a considerable fraction remains in the residual matrix. Vanadium is concentrated in the residual matrix in IN-731X but some is present in the γ' phase. Vanadium is not present in alloys 713C or 713LC. Columbium is concentrated practically entirely in the γ' phase in 713C and 713LC. Columbium is not present in IN-731X. Molybdenum is concentrated in the residual matrix in all three alloys to about the same degree although some is also present in the γ' phase. (The absolute molybdenum level is higher in alloys 713C and 713LC than in the IN-731X). Cobalt is concentrated in the residual

matrix in IN-731X but a considerable amount is found in the γ' phase. No cobalt is present in alloys 713C and 713LC. Chromium is preferentially partitioned in the residual matrix although some is also present in the γ' phase.

Thus it can be seen that there is considerable solution of alloy elements in the γ' phase. As a consequence, since the sigma phase developed in alloys 713C and 713LC is of the Ni-Cr-Mo type, it would seem possible for sigma to form from these regions also. A calculation for $\bar{N}_v$ for the γ' phase based on the chemistry in Tables VI and VII for alloys 713C and 713LC gives values of about 2.30 which is higher than for the residual matrix(2.20). Of course, there is considerably less Mo and Cr in the γ' than in the residual matrix so this would tend to limit the amount of sigma that could be formed from these regions. However, sigma is often observed in these alloys growing through γ' areas as shown in Figure 13. Such growth can easily be rationalized by the above argument whereas simply assuming γ' to be Ni_3 (Al, Ti, Cb, Ta) makes it difficult to see how this situation could exist.

CONCLUSIONS

1. No sigma is observed in IN-731X after long time testing in the region 1350-1900°F.

2. Coarse grain IN-731X has a higher rupture strength than fine grain in the region 1800-1900°F. At 1700°F fine grain IN-731X is somewhat stronger than coarse grain. In the 1350-1500°F range there is little effect of grain size on rupture strength.

3. Electron vacancy numbers obtained by using the actual γ' chemistry of IN-731X are less than those obtained by using simplified conventional calculations.

4. There is some variation in γ' chemistry of IN-731X after long time testing in the region 1350-1800°F, but the extent of the variation has little effect on electron vacancy number.

5. The beneficial effect of heat treatment in inhibiting sigma formation in alloys 713C and 713LC is attributed to homogenization and carbide precipitation upon heat treatment.

6. The detrimental effect of heat treatment on the 1500°F rupture properties of alloy 713C is attributed to grain boundary precipitation of γ' nucleated by carbide precipitation at the grain boundaries. This weakening effect overshadows any possible detrimental effect of sigma formation. It is possible that under some conditions sigma formation may actually enhance strength properties.

7. The beneficial effect of heat treatment on the 1500°F rupture properties of alloy 713LC is attributed to alteration of γ' morphology and lesser amount of carbide precipitation at grain boundaries upon heat treatment.

8. A simple method has been devised to estimate volume fraction of γ' phase in IN-731X, alloy 713LC and alloy 713C, knowing only the chemical composition of the γ' phase.

9. Electron vacancy calculations obtained by using γ' chemistry of alloys 713C and 713LC are higher than those obtained by using simplified conventional calculations. The amount of discrepancy is not as large as with IN-731X.

10. The γ' phase in IN-731X, alloy 713C and alloy 713LC shows extensive solubility for alloying elements including those involved in sigma formation. This circumstance

rationalizes the common observation that sigma phase often grows through γ' regions.

11. The γ' composition for IN-731X is $(Ni_{.884}\ Co_{.070}\ Cr_{.032}\ Mo_{.008}\ V_{.003})_3\ (Al_{.632}\ Ti_{.347}\ V_{.013}\ Cr_{.006}\ Mo_{.002})$

The γ' composition for alloys 713C and 713LC is $(Ni_{.980}\ Cr_{.016}\ Mo_{.004})_3\ (Al_{.714}\ Cb_{.099}\ Ti_{.048}\ Mo_{.038}\ Cr_{.103})$

JRM:DLP/klc

Copies to:
90
RSParmenter(77)
Technical Files(7)
RJRaudebaugh
RFDecker
CMDavis
CRCupp
DLPasquine
JRMihalisin

REFERENCES

1. J.R. Mihalisin, C.G. Bieber, R.T. Grant, "Sigma - Its Occurrence, Effect and Control in Nickel Base Superalloys," to be published.

2. H.J. Beattie, Jr., F.L. VerSnyder, "Microconsituents in High Temperature Alloys," Trans. ASM, Vol. 45, 1953, p. 397.

3. A. Taylor and R.W. Floyd, "The Constitution of Nickel-Rich Alloys of the Nickel-Titanium-Aluminum System," Journal Inst. of Metals 1952, Vol. 81, p. 25.

4. R.W. Guard and J.H. Westbrook, "Alloying Behavior of Ni_3Al (γ' phase)," Trans. AIME, Vol. 215, Oct. 1959, p. 807.

5. R.F. Decker and C.G. Bieber, "Microstructure of a Cast Age-Hardenable Nickel-Chromium Alloy," ASTM Spec. Tech. Publication No. 262, 1959, pp. 120-128.

APPENDIX I

REFERENCE METHOD FOR CALCULATION OF ELECTRON VACANCY NUMBER ($\bar{N}_V$ ref)

1. Convert the composition from weight percent to atomic percent.

2. After long time exposure in the sigma forming temperature range the MC carbides tend to transform to $M_{23}C_6$.

   a. Assume one-half of the carbon forms MC in the following preferential order: TaC, CbC, TiC.

   b. Assume the remaining carbon forms $M_{23}C_6$ of the following composition: $Cr_{21}(Mo, W)_2 C_6$ or $Cr_{23}C_6$ in the absence of Mo or W.

   c. If the weight percent of Mo + W > 6.0, then M_6C of composition $NiCo_2 (Mo, W)_3$ forms in place of $M_{23}C_6$.

3. Assume boron forms M_3B_2 of the following composition: $(Mo_{0.5} Ti_{0.15} Cr_{0.25} Ni_{0.10})_3B_2$

4. Assume gamma prime to be of the following composition: Ni_3 (Al, Ti, Ta, Cb, Zr, .03Cr*)

   * (0.03% of the original atomic percent)

5. The residual matrix will consist of the atomic percent minus those atoms tied up in the carbide reaction, boride reaction, and the gamma prime reaction. The total of these remaining atomic percentages gives the atomic concentration in the matrix. Conversion of this on the 100% basis gives the atomic percent of each element remaining in the matrix. It is this percentage that is used in order to calculate the electron vacancy number.

6. The formula for calculation of the electron vacancy number is as follows:

$$(\bar{N}_V \text{ ref}) = .66\ Ni + 1.71\ Co + 2.66\ Fe + 3.66\ Mn + 4.66\ (Cr + Mo + W) + 5.66\ V + 6.66\ Si$$

TABLE I

Composition of Heats (weight percent) and $\overline{N}_v$(ref) Numbers

IN-731X

Heat #	C	Cr	Co	Mo	V	Ti	Al	B	Si	Fe	Ni	$\overline{N}_v$
77	.16	9.60	9.72	2.46	.85	4.66	5.60	.014	.045	.23	66.936	2

Alloy 713C

Heat #	C	Cr	Mo	Cb+Ta	Al	Ti	B	Ni	Si	Fe	$\overline{N}_v$(
74	.13	12.94	4.46	2.21	6.14	.81	.010	73.300	.04	.10	2.
85	.11	13.23	4.46	2.09	5.86	.79	.009	73.451	.04	.10	2.

Alloy 713LC

Heat #	C	Cr	Mo	Cb+Ta	Al	Ti	B	Ni	Si	Fe	$\overline{N}_v$(
07	.06	12.32	4.46	2.13	5.90	.72	.009	74.401	.05	.20	2.
17	.03	12.52	4.41	2.10	5.90	.60	.009	74.431	<.10	.15	2.

TABLE II

Phases Electrolytically Extracted From IN-731X

Coarse Grain			Fine Grain		
Test Temp(°F)	Stress Rupture Results	Phases Present and Relative Abundance*	Test Temp(°F)	Stress Rupture Results	Phases Relativ
-	As Cast	MC(S-a_o = 4.30)	-	As Cast	MC(S-a_o
900	15,000 psi 126.3 hrs. 7.1 El. - 7.0 RA	MC(M-a_o = 4.29) $M_{23}C_6$(S-a_o = 10.67)	1900	15,000 psi 92.0 hrs. 7.1 El. - 11.7 RA	MC(MS-a_o $M_{23}C_6$(S-
	10,000 psi 512.2 hrs. 2.7 El. - 6.7 RA	MC(M-a_o = 4.29) $M_{23}C_6$(S-a_o = 10.68)		8000 psi 603.9 hrs. 2.1 El. -	MC(MS-a_o $M_{23}C_6$(S-
800	20,000 psi 264.7 hrs. 9.7 El. - 8.6 RA	MC(MS-a_o = 4.30) $M_{23}C_6$(S-a_o = 10.69)	1800	20,000 psi 194.2 hrs. 6.2 El. - 8.0 RA	MC(MS-a_o $M_{23}C_6$(S-
	15,000 psi 942.1 hrs. 5.3 El. - 7.1 RA	MC(MS-a_o = 4.30) $M_{23}C_6$(MS-a_o = 10.70)		15,000 psi 733.3 hrs. 7.1 El. - 13.7 RA	MC(MS-a_o $M_{23}C_6$(MS
700	40,000 psi 38.6 hrs. 4.5 El. - 7.0 RA	MC(S-a_o = 4.29) $M_{23}C_6$(MS-a_o = 10.67)	1700	40,000 psi 54.0 hrs. 8.9 El. - 7.8 RA	MC(MS-a_o $M_{23}C_6$(MS
	30,000 psi 184.0 hrs. 4.5 El. - 6.3 RA	MC(MS-a_o = 4.30) $M_{23}C_6$(MS-a_o = 10.69)		30,000 psi 263.4 hrs. 7.1 El. - 7.8 RA	MC(S-a_o $M_{23}C_6$(MS
	25,000 psi 547.7 hrs. 7.1 El. - 5.6 RA	MC(MS-a_o = 4.30) $M_{23}C_6$(MS-a_o = 10.69)		25,000 psi 612 hrs. 8.1 El. - 9.3 RA	MC(MS-a_o $M_{23}C_6$(MS
				20,000 psi 2102.4 hrs. 11.5 El. - 10.8 RA	MC(S-a_o $M_{23}C_6$(MS

Mihalisin T.F

TABLE II (Cont)

Coarse Grain			Fine Grain		
Test Temp(°F)	Stress Rupture Results	Phases Present and Relative Abundance*	Test Temp(°F)	Stress Rupture Results	Phases Pr Relative
1500	75,000 psi 12.6 hrs. 0.9 El. - 4.0 RA	MC(S-a_o = 4.30) $M_{23}C_6$(MS-a_o = 10.67)	1500	75,000 psi 109.4 hrs. 6.2 El. - 7.0 RA	MC(S-a_o = $M_{23}C_6$(MS-a
	60,000 psi 412.4 hrs. 2.7 El. - 6.2 RA	MC(S-a_o = 4.31) $M_{23}C_6$(MS-a_o = 10.70)		60,000 psi 481.8 hrs. 4.4 El. - 7.8 RA	MC(S-a_o = $M_{23}C_6$(MS-a
	50,000 psi 1515.7 hrs. 2.7 El. - 4.8 RA	MC(S-a_o = 4.31) $M_{23}C_6$(MS-a_o = 10.72)		50,000 psi 1925.6 hrs. 5.3 El. - 7.8 RA	MC(S-a_o = $M_{23}C_6$(MS-a
1350	100,000 psi 11.3 hrs. 1.8 El. - 6.6 RA	MC(S-a_o = 4.30) $M_{23}C_6$(VW-a_o = 10.72)	1350	100,000 psi 59.3 hrs. 1.8 El. - 3.0 RA	MC(S-a_o = $M_{23}C_6$(MW-a
	90,000 psi 198.7 hrs. 1.8 El. - 4.5 RA	MC(S-a_o = 4.31) $M_{23}C_6$(MW-a_o = 10.69)		90,000 psi 411.5 hrs. 2.7 El. 3.9 RA	MC(S-a_o = $M_{23}C_6$(M-a
				80,000 psi 2711.3 hrs. 4.4 El. - 6.3 RA	MC(S-a_o = $M_{23}C_6$(MS-a

Notes

S = Strong
MS = Moderate Strong
M = Moderate
MW = Moderate Weak
W = Weak
VW = Very Weak
a_o = in Å units

TABLE III

Chemical Analysis (Atomic Percent) of γ' Phase Extracted From As-Cast IN-731X

Cr	Co	Mo	V	Ti	Al	Ni	Vol % γ' calc	Vol % γ' obs	$(\bar{N}_V)$
3.09	5.91	.87	.57	8.28	15.33	65.60	58.9	58.4	2.07
±.03	±.07	±.01	±.06	±.53	±.37	±.21	± 3.8		±.04

TABLE IV

γ' Composition and Vol Percent, Residual Matrix Composition, $\bar{N}_V$ for IN-731X After Various Treatments

Treatment		Chemical Composition - Atomic Percent								Vol % γ' Calc	Vol % γ' obs	$\bar{N}_V$	γ' F
		C	Cr	Co	Mo	V	Ti	Al	Ni				
As Cast	γ'	.00	3.06	5.84	.87	.62	7.75	15.69	66.17	58.9	58.4		(Ni .880 Co .079
	R.M.*	.00	19.75	15.20	2.08	1.50	0.00	3.79	57.68			2.07	(Al .613 Ti .331
1350°F/ 2711.3 hrs	γ'	.00	2.49	4.61	0.80	0.76	8.40	16.03	66.91	57.8	56.7		(Ni .892 Co .062
	R.M.	.00	18.55	15.88	2.05	1.16	0.00	4.75	57.61			2.04	(Al .892 Ti .336
1500°F/ 1925.6 hrs	γ'	.00	2.40	4.96	0.59	0.39	7.80	17.05	66.80	62.6	60.6		(Ni .890 Co .070
	R.M.	.00	20.74	16.68	2.57	1.89	0.00	1.48	56.64			1.97	(Al .682 Ti .312
1800°F/ 733.7 hrs	γ'	.00	2.30	5.17	0.50	0.58	10.62	15.28	65.55	45.6	49.4		(Ni .875 Co .070
	R.M.	.00	14.88	12.71	2.02	1.24	0.00	8.09	61.06			2.10	(Al .590 Ti .410)

* R.M. = Residual Matrix

TABLE V

Stress Rupture Properties of Alloy 713C and Alloy 713LC

Heat #	Heat Treatment	Life (hrs) 1500°F/40,000 psi	Relative Amount of Sigma Present After Test	$\overline{N}_v$(r
		Alloy 713C		
74	As Cast	2182.7 hrs 8.0 Elong - 11.0 RA	Strong	2.1
74	2150°F/1 hr + 1900°F/4 hrs	1554.0 hrs 3.6 Elong - 3.0 RA	Moderate Strong	2.1
		Alloy 713LC		
07	As Cast	1604.0 hrs 7.1 Elong - 8.4 RA	Weak	2.0
07	2150°F/1 hr + 1900°F/4 hrs	2505 hrs 3.6 Elong - 7.0 RA	Nil	2.0
17	As Cast	1862.7 hrs 16.0 Elong - 27.8 RA	Nil	2.0
17	2150°F/1 hr + 1900°F/4 hrs	3648.6 hrs 12.0 Elong - 22.0 RA	Nil	2.0

Mihal
T.P.

TABLE VI

γ' Composition, Vol % γ', Residual Matrix Composition of Alloy 713C After Heat Treatment (Heat 85)

Treatment		Chemical Composition - Atomic Percent							Vol % γ' calc	Vol % γ' obs	$\bar{N}_v$	γ' Formula
		C	Cr	Mo	Cb	Al	Ti	Ni				
As Cast	γ'	.00	3.76	1.24	2.17	17.92	1.26	73.66	50.7	52.3		(Ni .982 Cr .014 Mo .004
	R.M.*	.00	23.36	3.86	.00	6.12	.31	66.30			2.20	(Al .717 Cb .087 Ti .050
2150°F/ 1 hr	γ'	.00	3.93	1.17	2.42	17.79	1.33	73.37	45.6	46.3		(Ni .978 Cr .018 Mo .004
	R.M.	.00	23.12	3.90	.00	6.21	.50	66.27			2.21	(Al .712 Cb .097 Ti .053
1900°F/ 4 hrs	γ'	.00	3.73	1.21	2.49	17.95	1.26	73.36	44.3	44.4		(Ni .978 Cr .018 Mo .004
	R.M.	.00	23.39	3.87	.00	6.05	.30	66.40			2.19	(Al .718 Cb .100 Ti .051
2150°F/1 hr + 1900°F/4 hrs	γ'	.00	3.85	1.15	2.45	18.04	1.30	73.20	45.0	45.3		(Ni .976 Cr .019 Mo .005
	R.M.	.00	23.26	3.94	.00	5.95	.26	66.60			2.18	(Al .722 Cb .098 Ti .052

* R.M. = Residual Matrix

TABLE VII

γ' Composition and Vol %, Residual Matrix Composition, $\bar{N}_v$ of Alloy 713LC

Heat 17

Treatment		Chemical Composition - Atomic Percent C	Cr	Mo	Cb	Al	Ti	Ni	Vol % γ' Calc	Vol % γ' obs	$\bar{N}_v$	γ' Formul
As Cast	γ'	.00	3.44	1.18	2.44	17.66	1.05	74.25	49.8	50.2		(Ni Cr Mo)3 .990 .008 .002
	R.M.*	.00	22.86	3.88	.00	6.60	.27	66.39			2.21	(Al Cb Ti C .706 .098 .042 .

Heat 07

As Cast	γ'	.00	3.82	1.35	2.66	17.90	1.12	73.17	45.1	46.2		(Ni Cr Mo)3 .976 .019 .005
	R.M.	.00	20.24	3.53	.00	7.41	.47	68.35			2.16	(Al Cb Ti C .716 .106 .045 .

* R.M. = Residual Matrix

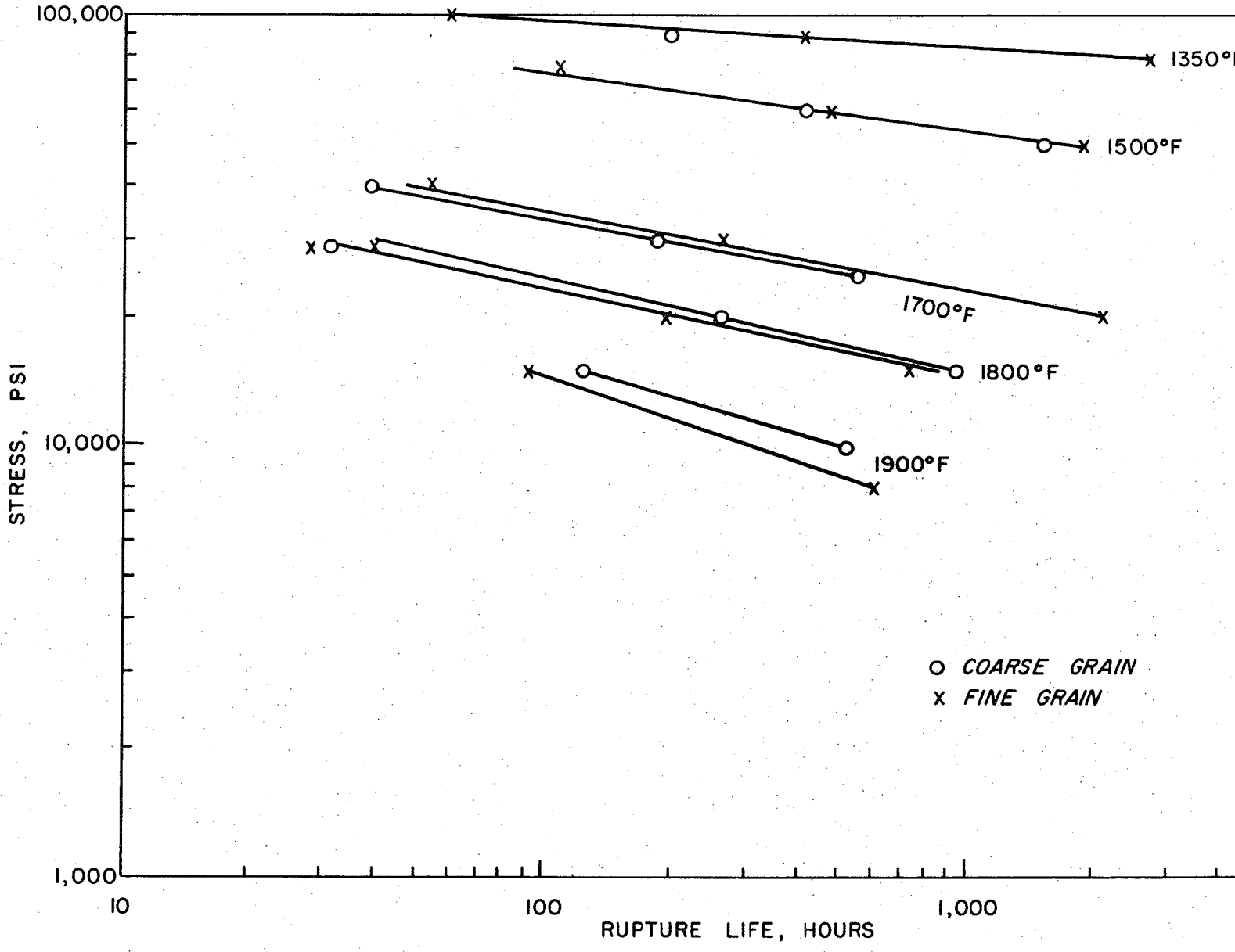

FIGURE 1- STRESS RUPTURE RESULTS ON IN-731X, AS-CAST CONDITI

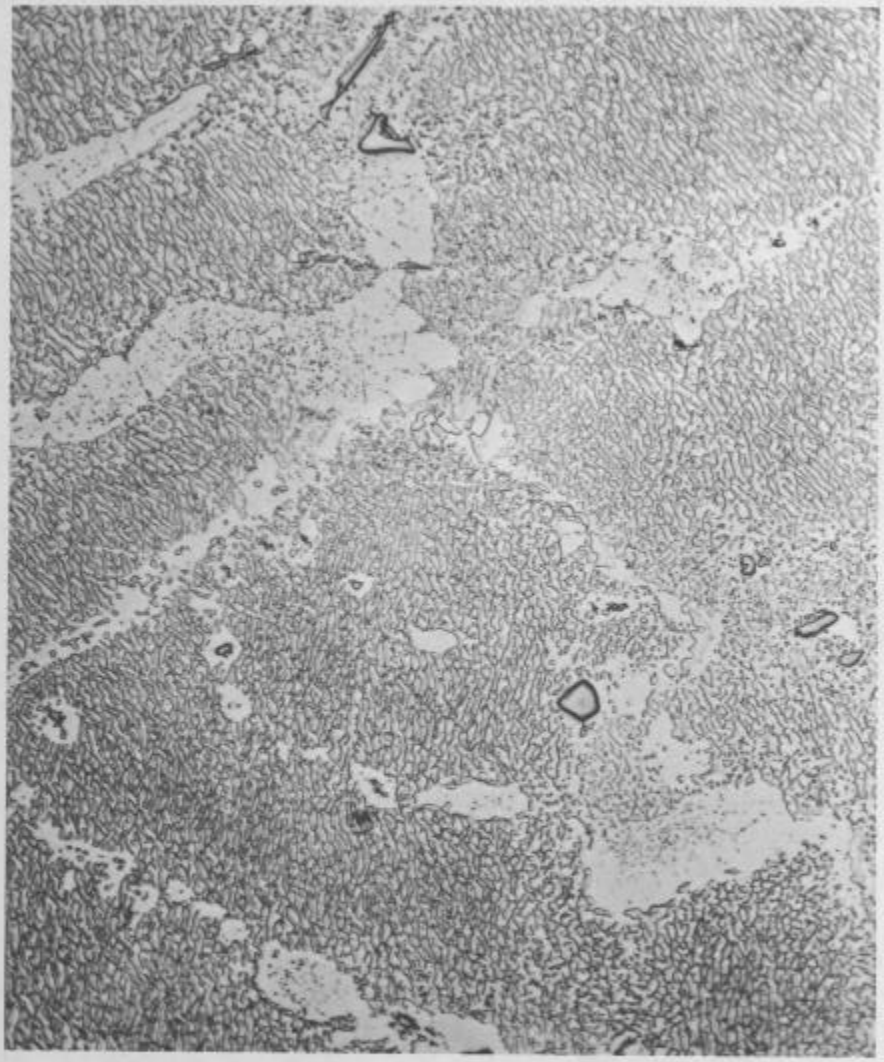

Fine grain - 1800°F/733.7 hrs. 500X
(a)

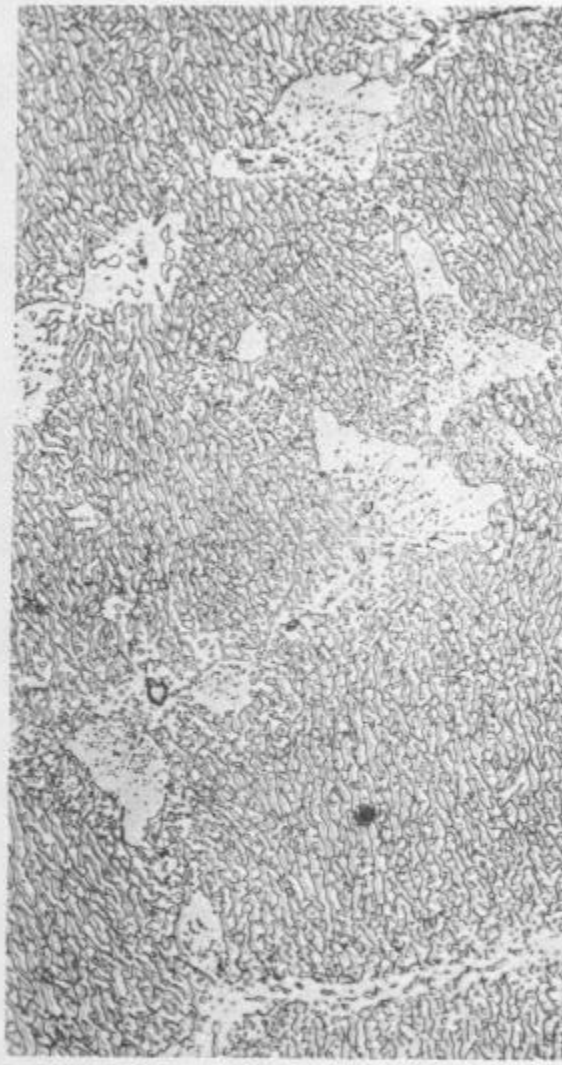

Coarse grain - 1800°F/942
(b)

Figure 2

Microstructure of IN 731X After Testing at 1800°F

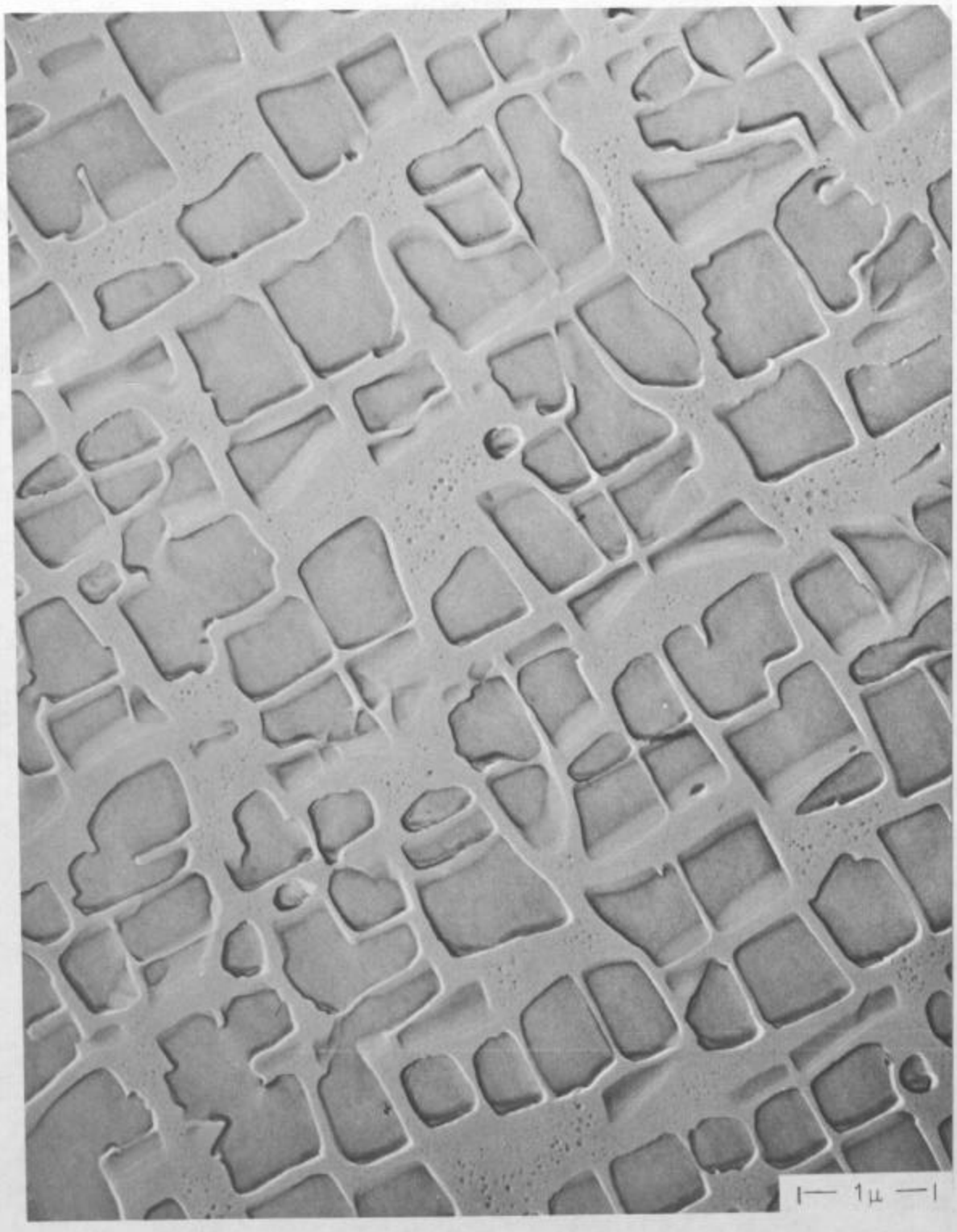

Figure 3

As Cast Microstructure of IN 731X

As Cast

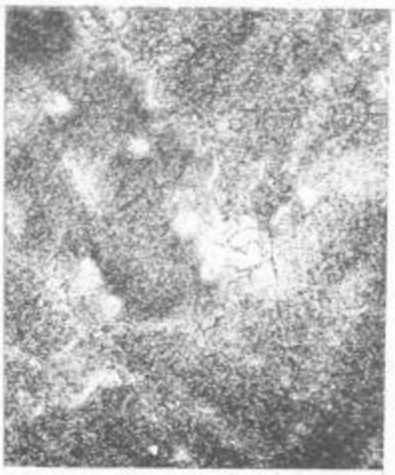

2150°F/1 hr.

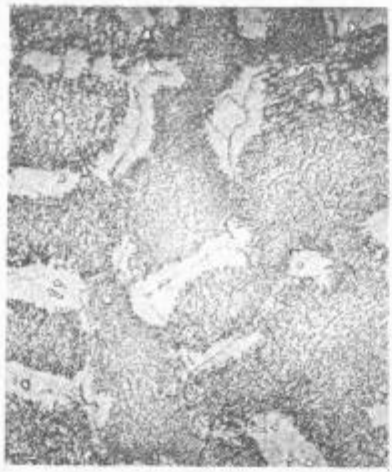

1900°F/4 hrs.

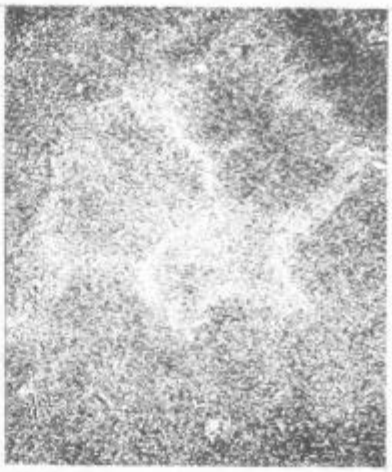

215

Phases Present and Relative Abundances* in Electrolytically Extracted Residues

As Cast	2150°F/1 hr.	1900°F/4 hrs.	215
MC(S-a_o = 4.40)	MC(S-a_o = 4.39) M_6C(W-a_o = 11.10)	MC(S-a_o = 4.39) M_6C(W-a_o = 10.86-11.13) $M_{23}C_6$(MS-a_o = 10.72)	

* S = Strong
MS = Moderate Strong
W = Weak
a_o = In Å Units

Figure 4

Effect of Heat Treatment on Microstructure(500X) and Phases Present in Alloy 713C(Heat 74)

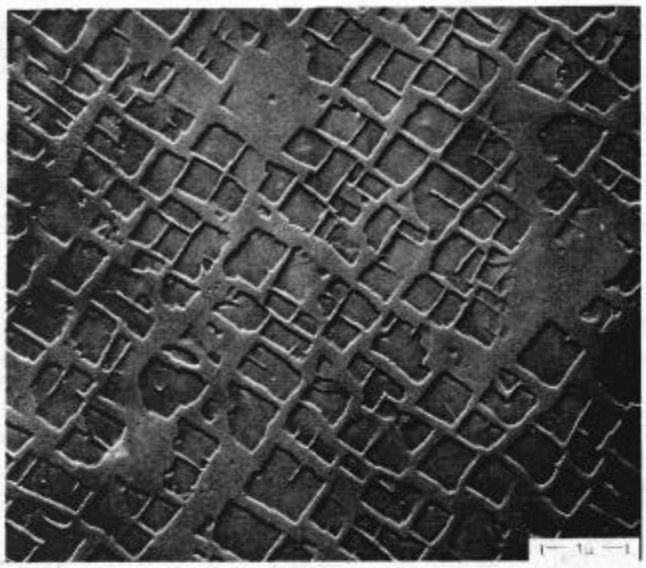

As Cast Area(a)

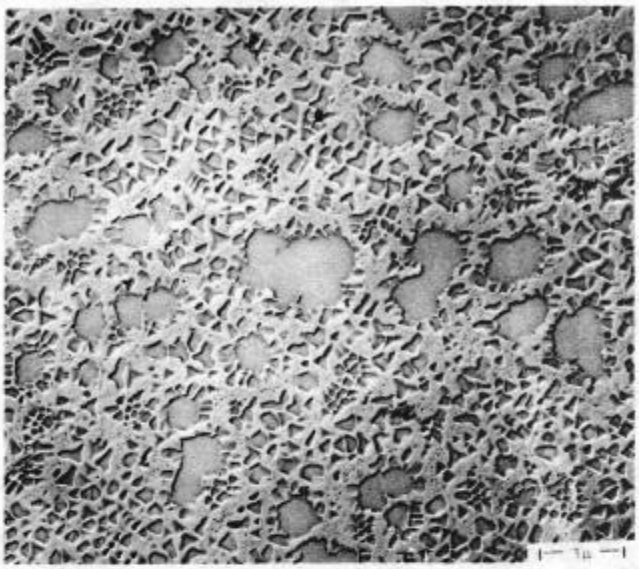

2150°F/1 hr. Area(b)

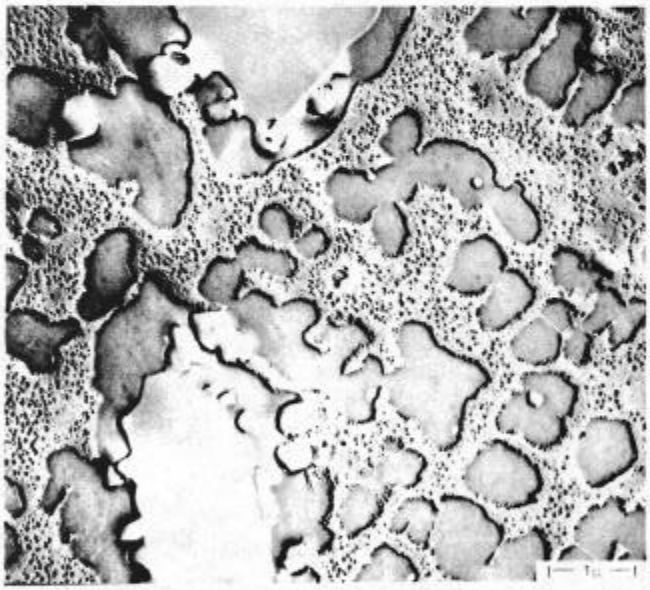

2150°F/1 hr. Area(c)

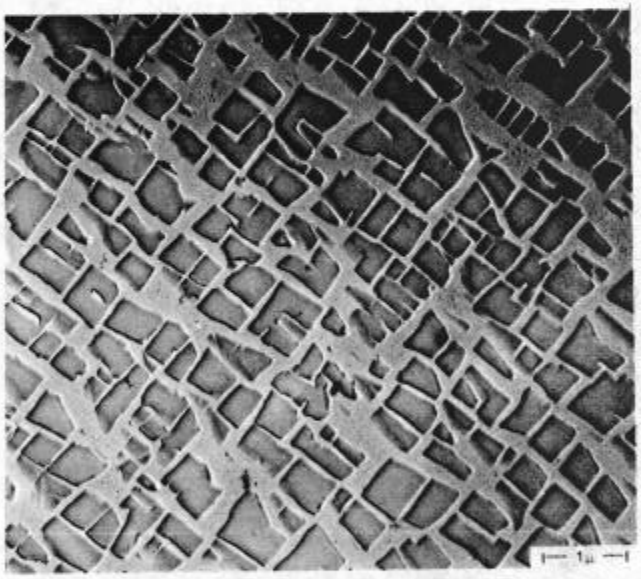

2150°F/1 hr. Area(d)

Figure 5

Microstructure of Alloy 713C
After Heat Treatment(Heat 74)

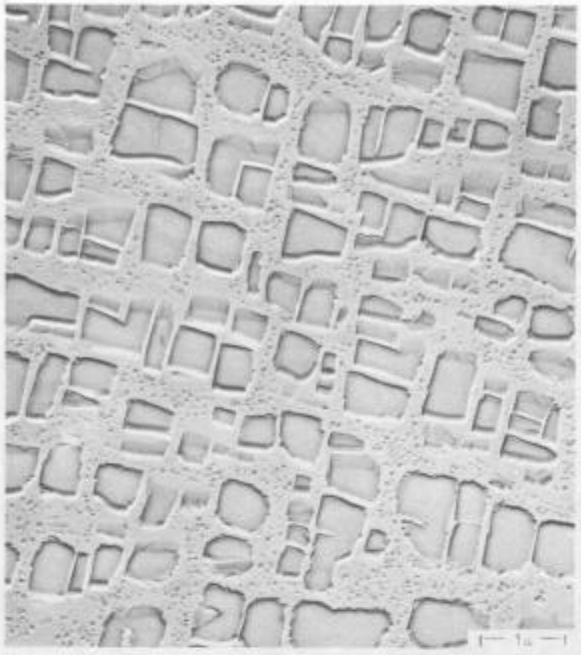

Area(a)

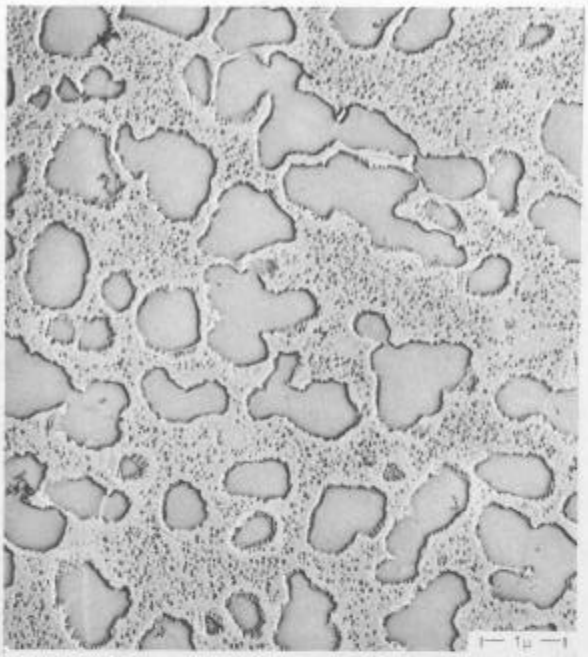

Area(b)

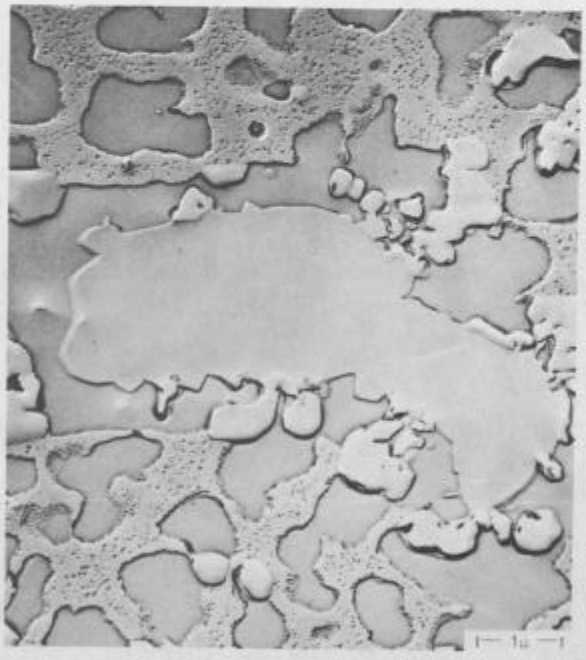

Area(c)

Figure 6

Microstructure of Alloy 713C
After 1900°F/4 hrs.(Heat 74)

Area(a)

Area(b)

Figure 7

Microstructure of Alloy 713C After 2150°F/1 hr. + 1900°F/4 hrs. - (Heat 74)

As Cast

2150°F/1 hr. + 190

Figure 8

Microstructure of Alloy 713LC After Heat Treatment(500X)-(Heat 17

As Cast

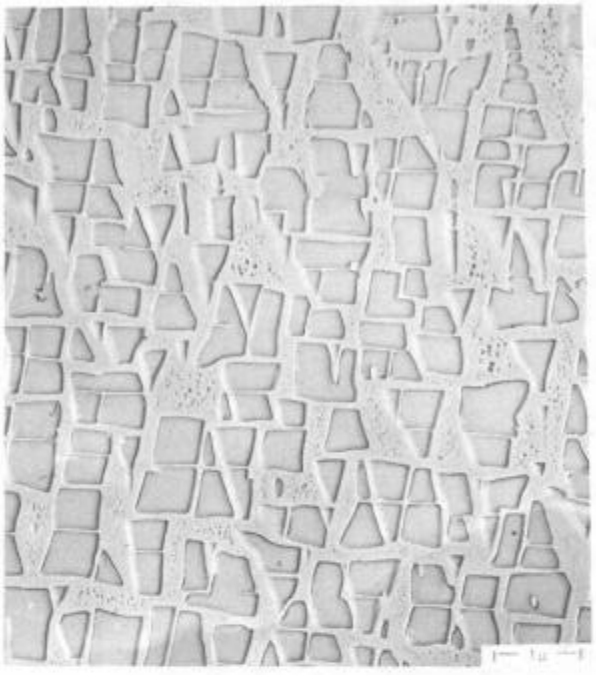

Area(a)

Area(b)

2150°F/1 hr. + 1900°F/4 hrs.

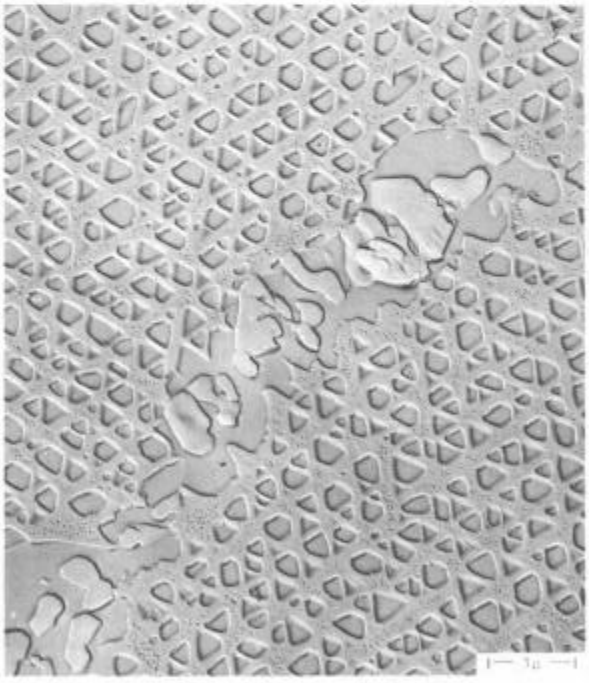

Area(c)

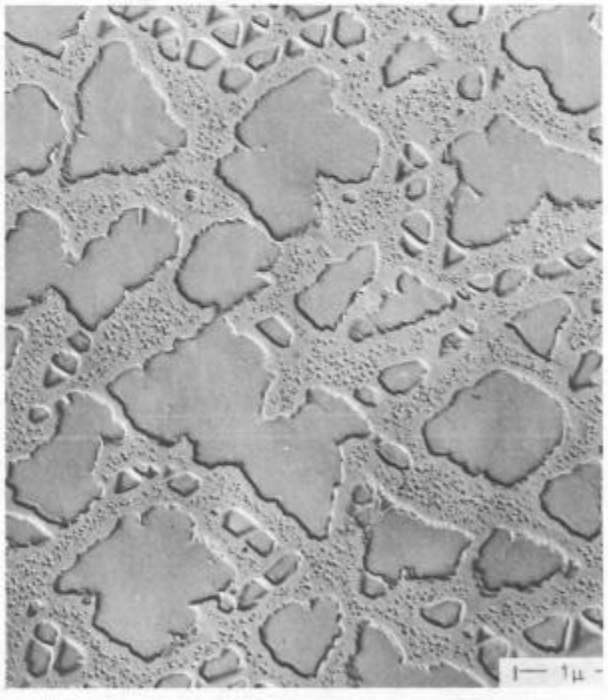

Area(d)

Figure 9

Microstructure of Alloy 713LC After Heat Treatment(Heat 17)

As Cast + 1500°F/ 40,000 psi - 2182.7 hrs. 8.0 Elong. - 11.0 R.A.	2150°F/1 hr (a.c.) + 1500°F/40,000 psi 1962.3 hrs. 5.3 Elong. 7.0 R.A.	1900°F/4 hrs(a.c.) + 1500°F/40,000 psi 1780.6 hrs. 4.0 Elong. 4.5 R.A.	2150°F/1 (a.c
		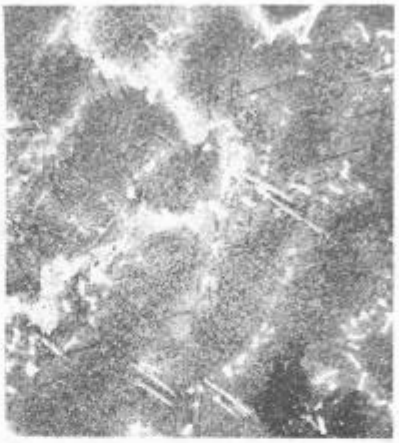	
MC(S-a_o = 4.39) $M_{23}C_6$(MS-a_o = 10.73) σ (S-a_o = 8.94) c/a = .517) M_6C(MW-a_o = 10.86-11.14)	MC(S-a_o = 4.39) $M_{23}C_6$(MS-a_o = 10.71) σ (MS-a_o = 8.94) c/a = .517) M_6C(MW-a_o = 10.93)	MC(S-a_o = 4.39) $M_{23}C_6$(MS-a_o = 10.73) σ (MS-a_o = 8.94) c/a = .517) M_6C(MW-a_o = 10.88-11.12)	M_2 M

Phases Present and Relative Abundances* in Electrolytically Extracted Resi

* S = Strong
MS = Moderate Strong
MW = Moderate Weak
W = Weak
a_o = In Å Units

Figure 10

Effect of Heat Treatment on Structure(500X) and Properties of Alloy 71

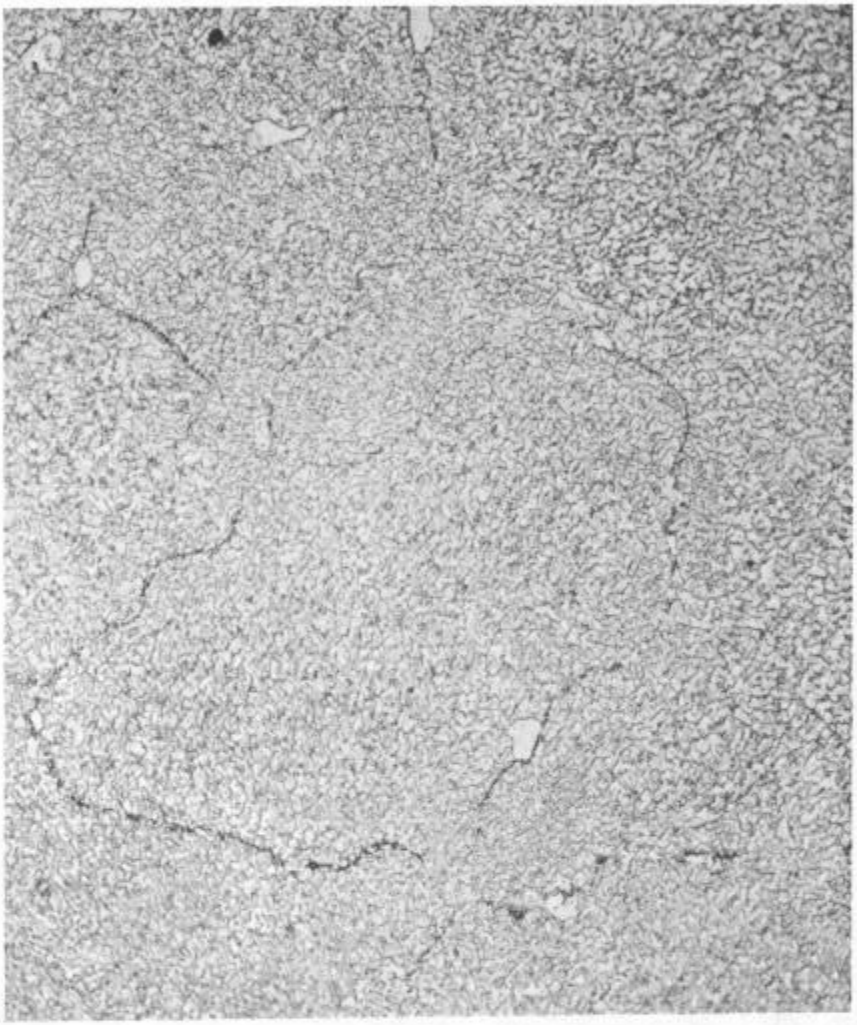

Figure 11

Microstructure of Alloy 713LC (500X) After 2150°F/1 hr. + 1900°F/4 hrs. (a.c.) + 1500°F/40,000 psi - 3648.6 hrs. 12.0 Elong. - 22.0 R.A.

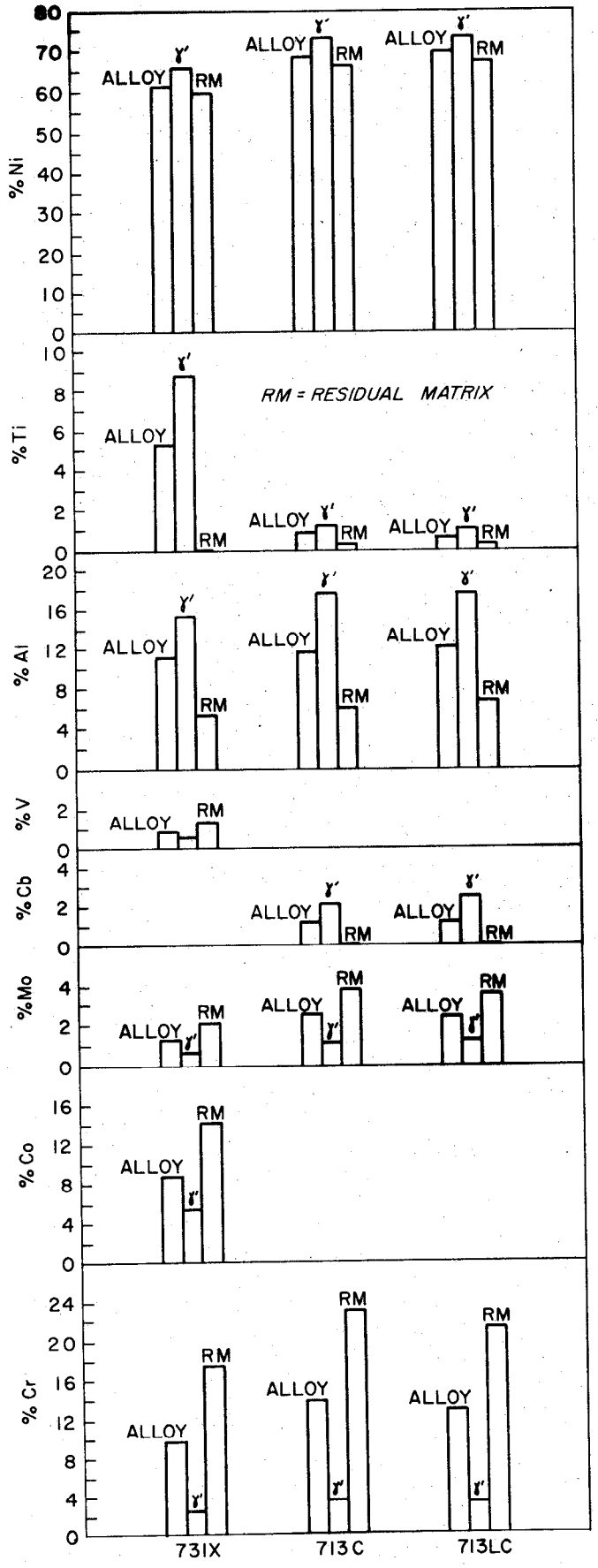

FIGURE 12 – PARTITIONING OF ALLOY ELEMENTS BETWEEN γ′ AND RESIDUAL MATRIX FOR IN-731X, ALLOY 713C AND ALLOY 713LC.

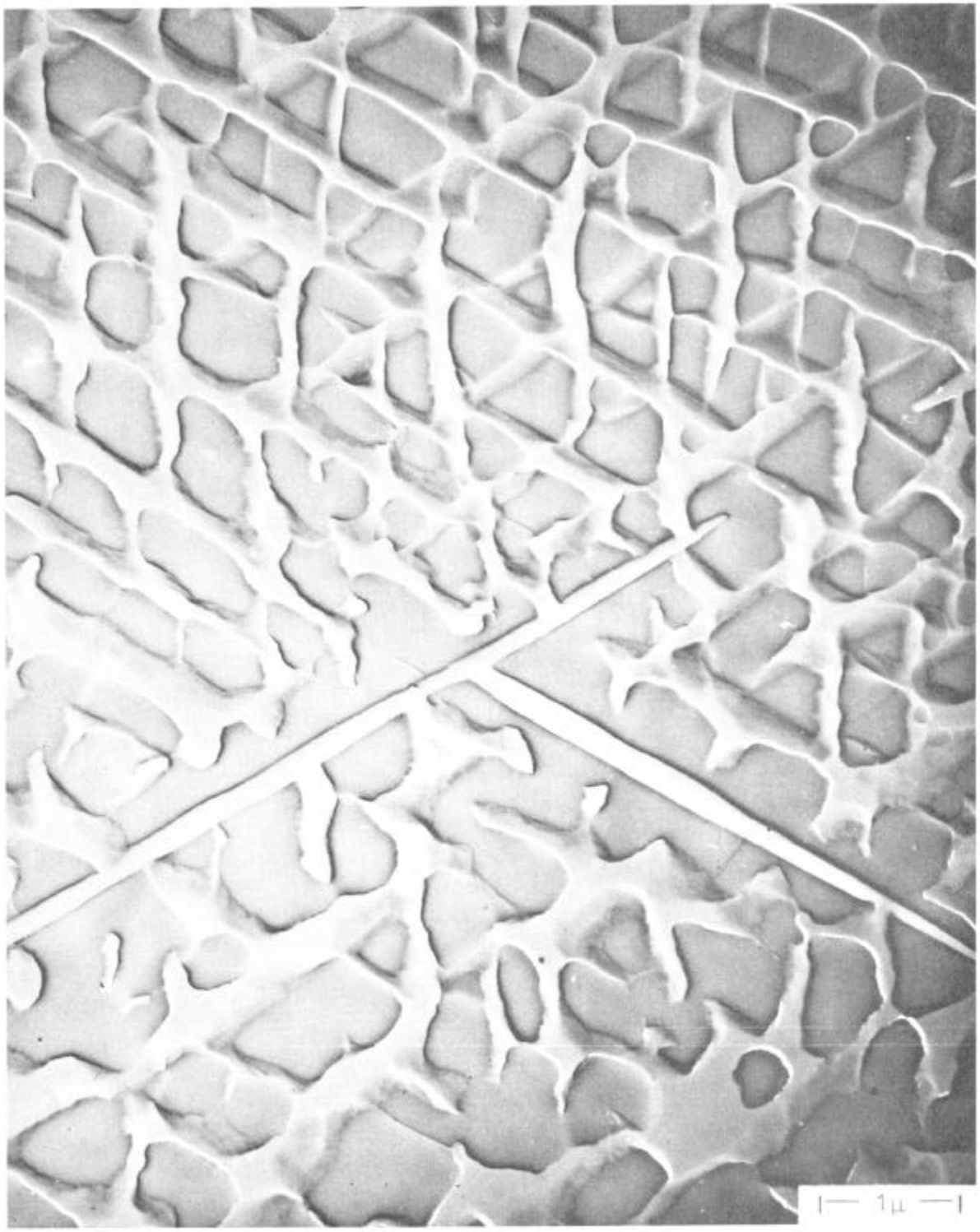

Figure 13

Sigma Formation in Alloy 713C - Heat 74 - 2182.7 hrs./40,000 psi/1500°F